Dear author,

In the stage of preparing your full work for evaluation, after receiving approval of the corresponding abstract, we kindly ask you to follow the next steps:

1. Update your approved abstract (you might want to introduce modifications) and submit it now in a written version according to the abstract template (many abstracts were introduced directly into the websystem). This version of the abstract will compose the *abstracts booklet* to be distributed to the participants when registering;

2. Fill the form in the next page, indicating to which section you would like your work to be directed. This will help organizing the sessions according to the mini-symposia advertised rather than in the areas and subareas present in the websystem. We apologize for this possible confusion. The reason is that we are using the websystem provided by ABCM, which does not allow us to introduce thematic sessions freely.

If any doubts arise, please contact us.

Your presence in MecSol 2017 will help making this a very successful event. We look forward to seeing you in Joinville!

With kind regards,

The Organizing Committee
MecSol 2017

6th International Symposium on Solid Mechanics

Click on the box to select the Mini-Symposia:

☐ Multiaxial and Fretting Fatigue (*Edgar Mamiya* and *Lucival Malcher*);

☒ Composite Materials (*Ricardo de Medeiros*);

☐ Constitutive Models I – Plasticity and Damage (*Lucival Malcher*, *Miguel Vaz Jr.* and *Edgar Mamiya*);

☐ Constitutive Models II – Viscoelastic and Viscoplastic Solids: Models and Applications (*Heraldo Mattos*);

☐ Impact Engineering (*Marcílio Alves*);

☐ Structural Reliability Methods and Reliability-Based Design Optimization (*André Beck*);

☐ Topology Optimization of Multifunctional Materials, Fluids and Structures (*Eduardo Lenz Cardoso* e *Emilio Carlos Nelli Silva*);

☐ Topological Derivatives: Theory and Applications (*André Novotny*);

☐ X-FEM, G-FEM and Meshfree Methods (*Roberto Dalledone Machado* and *Rodrigo Rossi*);

☐ High Order Finite Elements (*Marco Lúcio Bittencourt*);

☐ Nonlinear Analyses (*Eduardo Campello*);

☐ Other section;

MECSOL Joinville 2017

April 26-28, 2017
Joinville, Santa Catarina, Brazil

Structural Health Monitoring for Sandwich Structures

Denys E. T. Marques
Aeronautical Engineering Department
São Carlos School of Engineering, University of Sao Paulo
denys.marques@usp.br

Felipe R. Flor
Aeronautical Engineering Department
São Carlos School of Engineering, University of Sao Paulo
feliperendeiro88@gmail.com

Ricardo de Medeiros
Mechanical Engineering Department
College of Technological Sciences, Santa Catarina State University
ricardo.medeiros@udesc.br

Carlos do Carmo Pagani Junior
Aeronautical Engineering Department
São Carlos School of Engineering, University of Sao Paulo
paganni.carlos@gmail.com

Volnei Tita
Aeronautical Engineering Department
São Carlos School of Engineering, University of Sao Paulo
voltita@sc.usp.br

ABSTRACT

This work aims to contribute for the development of SHM systems based on vibration methods to be applied on sandwich structures. The main objective is focused on the damage identification. Specimens of a sandwich structure made of skins in epoxy resin reinforced by glass fiber and a core of PVC foam are manufactured. First, finite element models are developed in order to analyze the dynamic characteristics of undamaged and damaged structures with presence or not of two piezoelectric sensors. Then, vibration experimental analyses are performed on undamaged specimens of sandwich structures. The mode shapes and natural frequencies are compared to the computational results. Second, vibration experimental analyses are carried out on undamaged and damaged specimens of sandwich structures with piezoelectric sensors or not. Finally, a traditional damage metric is calculated based on Frequency Response Functions obtained from computational and experimental analyses. However, this work brings a new procedure in order to improve the quality of results provided by this damage metric. By one hand, the damage metric values showed that the new procedure is effective to identify the damage using both amplitude and phase experimental data. By the other hand, for computational analysis, the damage metric values are not effectives, because the finite element models were not able to simulate the dynamic behavior of the sandwich structures.

Keywords: Structural Health Monitoring, Sandwich Structures, Vibration Methods, Finite Element Analysis, Experimental Analysis.

1 INTRODUCTION

Composite sandwich structures consist of two outer layers, or skins, generally thinner and made of a rigid material, which surround a core of low stiffness, generally thicker and of lower density. The resulting structure has low density, high flexural stiffness and high sound insulation, which made these structures widely used in the aeronautical industry [1,2]. Together with the increase in its use came the necessity of a method to monitor its structural integrity. The starting point of any Structural Health Monitoring system (SHM) is the initial damage detection to the structure. For this purpose, one of the most used method is based on the vibrational response of the structures.

The physical principle behind a SHM system based on vibrational analysis is that modal parameters such as natural frequencies, vibration modes or damping are functions of the structure properties (its rigidity, damping, etc.). Thus, changes in these structural parameters resulting from structural damage (such as delaminations, cracks, etc.) would reflect as a change in modal parameters [3].

It can be found in the literature some examples of successful application of this principle to estimate and locate damage in sandwich and composite structures [4-6]. In 2005, Lestari and Qiao [7] used smart sensors to perform damage detection, location and quantification of damage based on curvature mode shapes. The authors used honeycomb sandwich beams made of glass fibers and polyester resin with the core in corrugated cells damaged and undamaged. In 2010, Amir *et al*. [8] used the dynamic response of a honeycomb sandwich structure to detect multi-site damage. The authors determined variation of natural frequencies and variation of damping ratio to estimate the damage. The studies concluded that damping ratio was more reliable than natural frequency. The researchers also discussed how low impact damage, such as dropped tools during maintenance, can cause small indentations in the structure. They highlighted that the use of natural frequency for detecting damage cannot reliably detect initial damages on the structures. Thus, for composite structures, the interest by the academy over the use of modal damping variation has increased since this criterion is more sensible to damage than stiffness. Dhamande and Bhaskar [9] made use of the first three natural frequencies and mode shapes to detect and localize two types of damage - debonding and core crushing - in a honeycomb sandwich beam, which has core in aluminum and skins in carbon fiber reinforced plastic.

Based on the scenario approached above, this present work will also focus on SHM for sandwich structures based on difference of Frequency Response Functions aided by a traditional metric for damage identification. However, this work brings a new procedure in order to improve the quality of results provided by this damage metric.

2 MATERIALS AND METHODS

2.1 Sandwich structures specimens: Materials and sensors

The sandwich structures were made of glass fiber/epoxy skins and PVC foam core. The specimens have three output regions, one input point and one damage area. The dimensions for the specimens are displayed in Figure 1. As noted in the schema, the positions 2 and 3 have accelerometers or Macro Fiber Composite (MFC) piezoelectric sensors. Position 4 is the area of

damage (debonding), which was obtained by replacing the adhesive component by a teflon^{TM} layer through the overlap area. Lastly, position 5 has always an accelerometer, which is considered as a reference point.

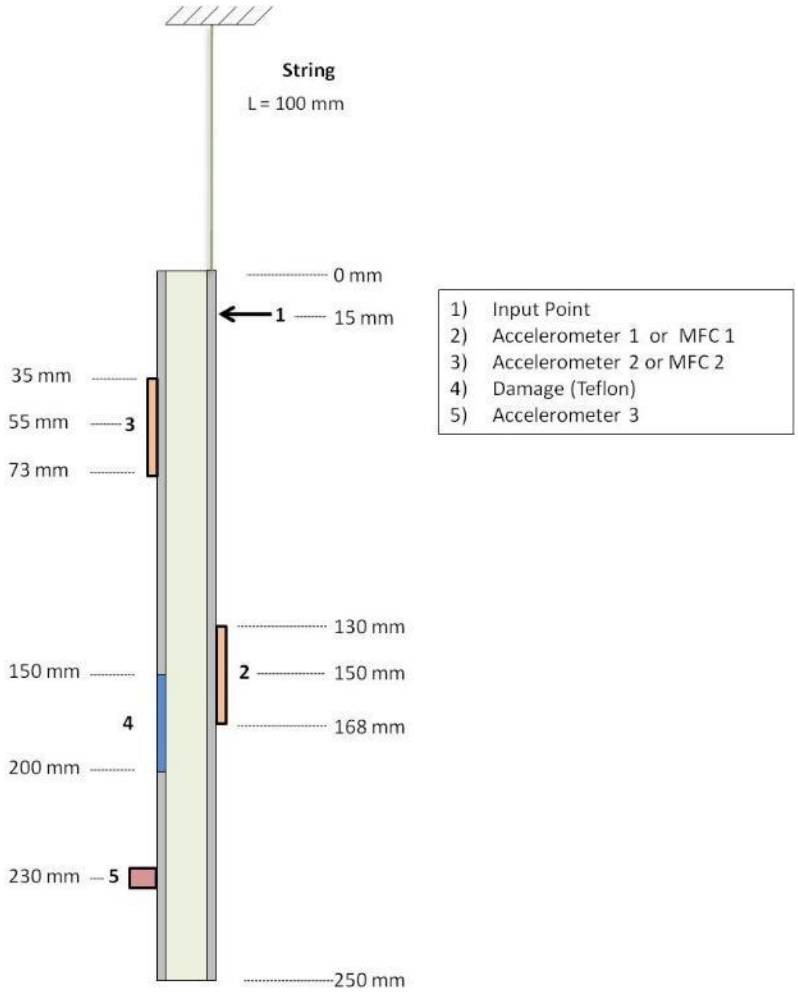

Figure 1: Sandwich structures specimens.

The skin was a laminate made of unidirectional glass fibers and epoxy Araldite Ly 1564 BR resin catalyzed by REN Hy 150 BR. The plies were stacked as $[0°, +45°, -45°]_S$ configuration. This composite material was manufactured at Laboratory of Aeronautic Structures (University of São Paulo). They were produced by laying up dry fibers on top of a flat glass mold in accordance to the stacking sequence. The resin was applied by using vacuum system and it was cured under 25ºC for 12 hours. The mechanical properties of the skins were not obtained experimentally, for that reason, values used in the computational analyses were found in the literature [10]. These values are shown in Table 1.

Table 1 Skin Properties [10]

Properties	Unit	Value
E_{11}	GPa	44.80
E_{22}	GPa	11.30
E_{33}	GPa	11.30
G_{13}	GPa	4.86
G_{23}	GPa	4.45
G_{12}	GPa	4.86
ν_{12}	-	0.28
ν_{13}	-	0.28
ν_{23}	-	0.28
ρ	kg/m^3	1580

The core was made of PVC foam H60 from Divinicell, which is commonly used by the aeronautical industry. In fact, the elastic properties and strength values under tension and compression were determined by Caliri Junior *et al.* [11-13] and are shown in Table 2.

Table 2 PVC Foam Core Elastic Properties [11-13]

Properties	Unit	Value
E_{11}	GPa	0.034
E_{22}	GPa	0.034
E_{33}	GPa	0.112
G_{13}	GPa	0.02
G_{23}	GPa	0.02
G_{12}	GPa	0.0139
ν_{12}	-	0.22
ν_{21}	-	0.22
ν_{13}	-	0.35
ν_{31}	-	0.11
ν_{23}	-	0.35
ν_{32}	-	0.11
ρ	Kg/m^3	60.00

The piezoelectric sensor used for monitoring the sandwich structure was the MFC M2814-P1 by Smart Material Corp. The properties of this component were obtained by Sartorato *et al.* [14] and Medeiros [15] and are shown at Table 3.

Table 3 Piezoelectric Sensor Properties (M2814-P1) [14,15].

Properties	Unit	Value
C_{11}	GPa	1.47
C_{12}	GPa	1.19
C_{13}	GPa	1.22
C_{33}	GPa	59.70
C_{44}	GPa	23.20
C_{66}	GPa	0.28
e_{13}	C/m^2	-0.05
e_{15}	C/m^2	0.17
e_{33}	C/m^2	21.07
ϵ_{11}	nF/m	0.62
ϵ_{33}	nF/m	15.40
ρ	Kg/m^3	5440

Lastly, the skins (two laminate plates) were jointed to the core by using the same epoxy resin used for the skins. This bonding process was performed inside a kiln for 8 hours at the temperature of 65ºC. This sandwich plate was then carefully cut into four specimens of sandwich beams with dimensions about 25 mm of width and 12 mm of thickness. Therefore, four damaged and undamaged specimens were investigated. The specimens analyzed are identified in accordance to the following code:

- S1: Intact (Undamaged) specimen
- S2: Damaged specimen
- P0: Absence of MFC (Output by: "A1", "A2", "A3")
- P1: Presence of one MFC (Output by: "P1", "A2", "A3")
- P2: Presence of two MFCs (Output by: “P1”, “P2”, “A3”)

Where “A” corresponds to accelerometer and “P” corresponds to MFC sensor. Besides, “1” is related to the position 2 (Fig. 1), “2” is related to the position 3 (Fig. 1) and “3” is related to the position 5 (Fig. 1).

2.2 Experimental Set-ups and Instrumentation

The vibration tests were limited to the free-free boundary condition. In order to achieve this, the specimens were connected to a metal support via a thin string.

The data was acquired by using LMS SCADAS Mobile, which was set to cover a bandwidth of 4096 Hz with 8193 spectral lines. The apparatus was set to compute the mean values out of 5 repetitions to reduce random fluctuations or noise and only data with reasonable high coherence values for the range of interest was used.

Besides the piezoelectric sensor previously mentioned, data acquisition was also performed by using three accelerometers Piezotronics Model 352C22, which had the sensitivities of 9.57 mV/g, 9.31 mV/g and 99.6 mV/g. The input load was performed by using an impulse force Piezotronics

hammer Model PCB 0860C3. Figure 2 shows details about the input point (position 1) and location of accelerometer 1 ("A1" – position 2).

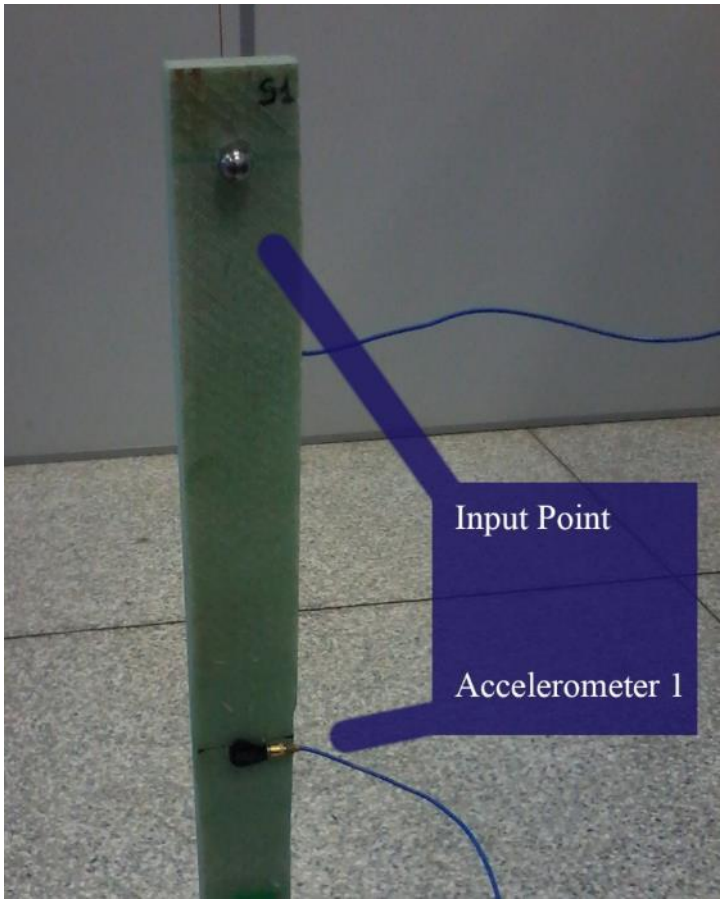

Figure 2: Details of the experimental set-up for free-free condition of sandwich structure: input and output points (Flor [16]).

2.3 Experimental Procedures

The experimental procedures were conducted in the following order: the first analysis compared the dynamic response of the specimens S1P0, S1P1 and S1P2 in order to verify the influence of the presence of the piezoelectric sensor. The second one compared the dynamic response of the specimens S1P0 and S2P0 in order to verify the influence of the presence of damage in the sandwich structure. The third analysis compared the dynamic response of specimens with MFCs in order to verify the possibility of using their dynamic signature to identify the damage.

3 DAMAGE METRICS

In this work, the damage was initially quantified by using the damage metric presented by Mickens *et al.* [17]. This method uses the magnitudes of the FRFs of both the intact (undamaged)

and damaged structures, and the damage factor (DF) can be calculated by the following equations (1) and (2):

$$y(f) = \left| \frac{|H^i| - |H^d|}{|H^i|} \right| \tag{1}$$

$$DF = \frac{\Delta f}{f_2 - f_1} \sum_i^n y_i\,(f) \tag{2}$$

Where H^i and H^d are the FRF amplitudes of undamaged (intact) and damaged structure, respectively, for a certain frequency range $[f_1, f_2]$ and certain frequency increment Δf. However, the damage metric can be also calculated as shown by Equations (3) to (5):

$$\phi^x = Tan^{-1}\left(\frac{Im(H^x)}{Real(H^x)}\right);\ \ x = i, d \tag{3}$$

$$y(f) = \left| \frac{|\phi^i| - |\phi^d|}{|\phi^i|} \right| \tag{4}$$

$$DF = \frac{\Delta f}{f_2 - f_1} \sum_i^n y_i\,(f) \tag{5}$$

Where ϕ is the FRF phase angle value of undamaged (intact) and damaged structure for a certain frequency range $[f_1, f_2]$ and certain frequency increment Δf, as well.

3.1 Proposed Procedure

The damage metric proposed by Mickens is strictly based on the relative differences of magnitude between the dynamic signatures of the intact (undamaged) and damaged specimens. This procedure includes one particular issue. The damage factor has a tendentious behavior because of its choice to use the FRF of the intact specimen in the denominator. When H^i approaches zero, the value of $y(f)$ can become unreasonably high, even when the absolute difference between H^i and H^d is small. The same behavior can be also observed when applying Mickens' method into phase data. Figure 3 shows an example from an experimental result where the low values of H^i produce a high contribution to damage at a frequency range that has actually no damage.

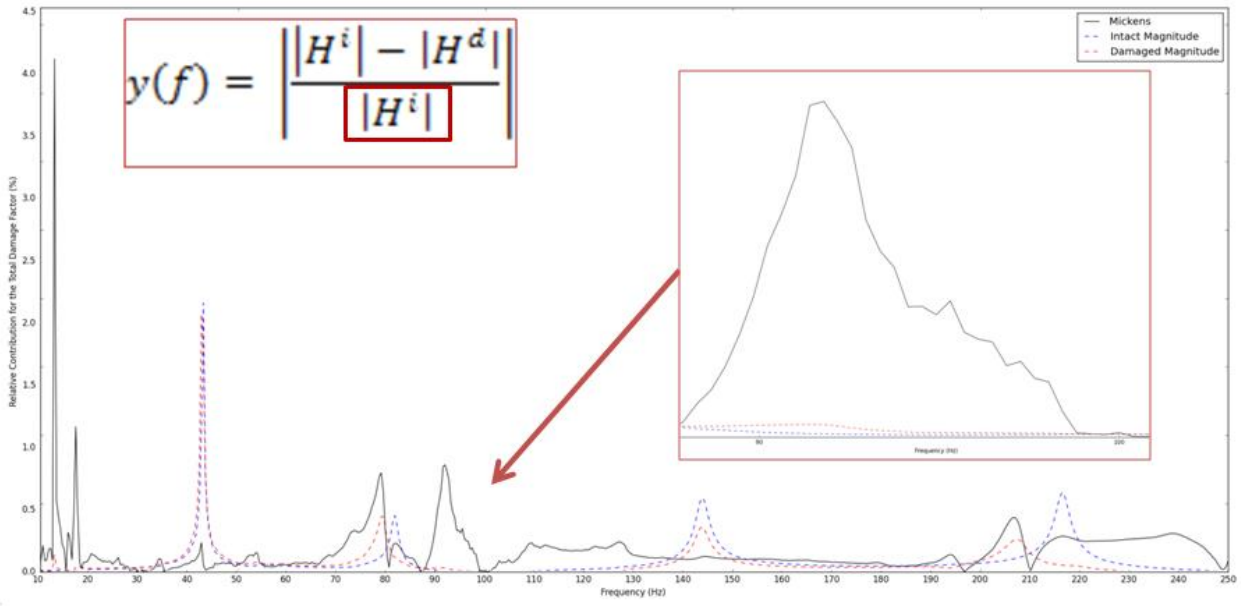

Figure 3: Mickens' damage metric - Low value divisions.

To solve this issue, a procedure was proposed. Thus, two modifications should be implemented into the metric. The first step consists on the implementation of a filter that reduces the occurrences of small denominators in the calculations. This filter operates on both the intact and damaged FRFs. This is achieved by the following procedure:

- The third quartile of the data is automatically accepted as the default. To obtain the third quartile, it is necessary to first arrange the values of the array in crescent order. The third quartile corresponds to the value between the median and the highest value of the array. In other words, given an array with *n* elements, if this array is arranged in crescent order, the third quartile will be the value stored at the 0.75*n element.
- The values bellow the third quartile are only considered if their magnitude is greater than 15% of the highest value of the data. This step prevents data of reasonable magnitude to be ignored in systems that contain a low standard deviation.
- A range will only be ignored if it has been filtered in both the intact and damaged curves. By the end of the process, the filter can accept a number of values that cover from 25% up to 100% of original data. A value will be only ignored during the damage metric calculation, if it is in a filtered frequency for both the intact and damaged FRFs. The overall result of this process is displayed in Figure 4.

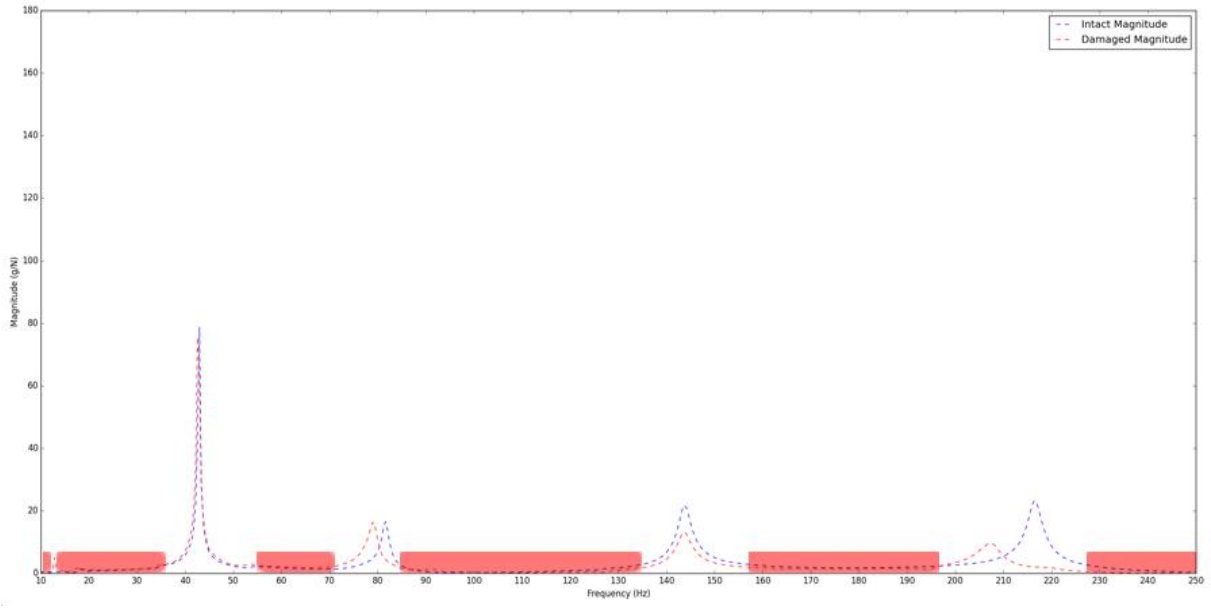

Figure 4: Filtering of specific frequency ranges of the data.

The next step has the purpose of solving the issues with the tendentious behavior of the damage contribution. This is solved by changing the denominator of the Equation (1) to $\min(H^i, H^d)$ or $\max(H^i, H^d)$. The modified damage metric applies $\max(H^i, H^d)$ values in order to avoid divisions by small numbers, which provide high values for damage metric.

4 FINITE ELEMENT ANALYSIS

The simulations for the sandwich structures were performed using the commercial software package ABAQUS™. The skins were modeled by a total of 600 shell elements (S4R), which is a 4-node shell element, while the core and MFCs sensors were modeled by solid elements. The core was meshed with 2000 C3D8R type elements, which is an 8-node linear brick for 3D stress analyses, and the MFCs were meshed with 660 C3D20RE type elements, which is a 20-node quadratic brick with mechanical and dielectric degrees of freedom. It is important to highlight that a mesh sensibility analysis was performed in order to verify variation of results from modal analyses. The first models were developed by using 2600 elements, which were compared to second ones with a more refined mesh (9500 elements). After this investigation, it was observed only a very small variation between natural frequencies (less than 2%), showing that it was not required to use more refined mesh.

The glue was simulated linking the skin to the core by using the "tie" algorithm implemented at ABAQUS™. Hence, the glue is considered perfect and not deformable, with no thickness. The damage was defined simply as a region without the tie constraint, allowing the surfaces to separate freely. The free-free boundary condition of the specimen was simulated by using the engineering feature "spring". Figure 5 shows specimen S2P2 (which contains both the damage and the MFC elements).

The dynamic analyses were performed via the "Steady-State Dynamics Modal". This step solution was preceded by the "Frequency" step, which calculates the eigen frequencies for the non-

transient condition. The eigenproblem was solved using Lanczos eigensolver, which is implemented in Abaqus. The experimental damping factors were included in order to improve the numerical models. The damping factors used were obtained by approximating the modal peaks of the experimental FRFs into independents second order transfer functions. Therefore, each transfer function had a single natural frequency and a single damping factor associated to it. This procedure was made using Matlab^{TM} and frequency domain identification tools.

It is important to highlight that this FE model was a preliminary computational investigation, and it was developed in order to provide a simple prediction of the dynamical behavior of the real structure, aiding the experimental analysis and vice-versa. In fact, non-damped analyses could predict the range of frequencies to be investigated in the experimental tests, and the damped analyses were carried out in order to simulate the real structure with the smart sensors.

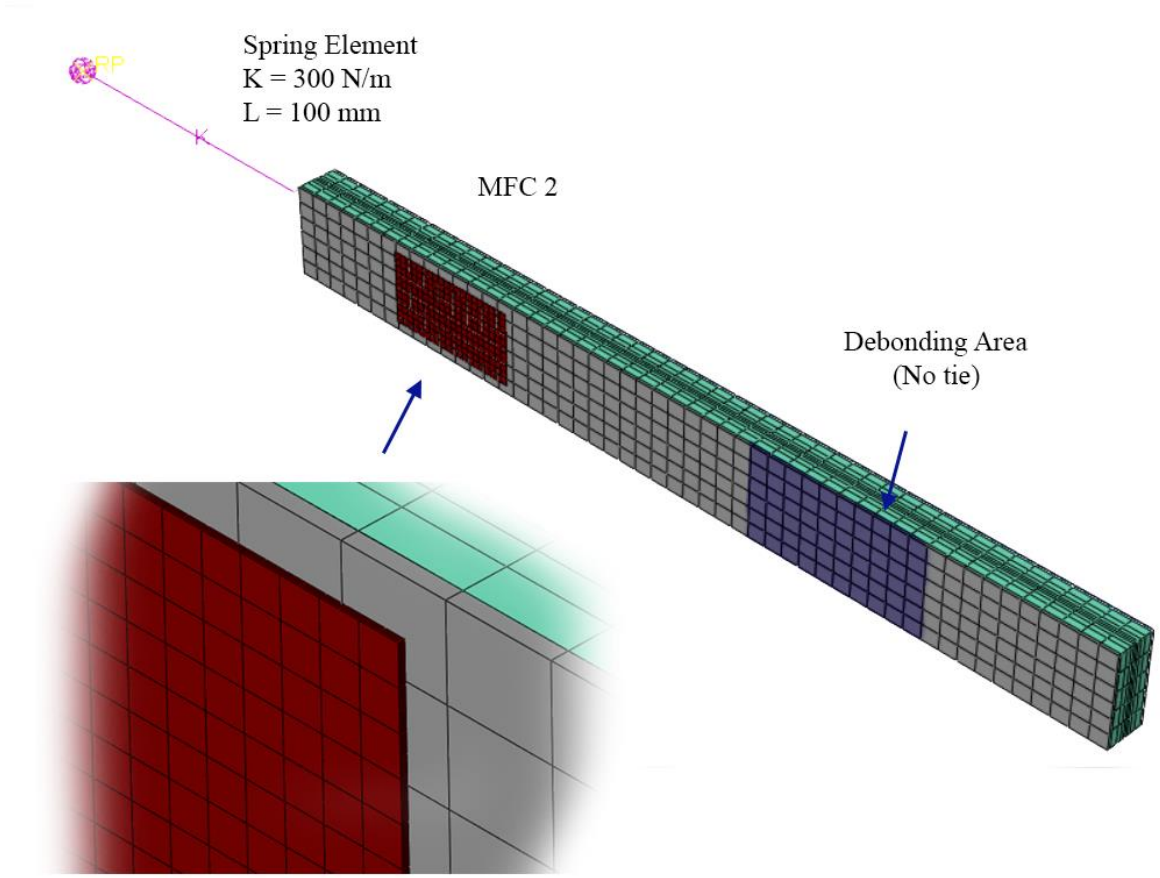

Figure 5: Finite Element model for the sandwich structure S2P2.

5 RESULTS

After performing the experimental analysis at frequency range [0,4096] Hz, it was necessary to define a more restricted range, considering the possible limitations of the experimental method

used. Besides, for the purposes of this study, the range of interest needs only to involve the first non-rigid vibration modes of the specimens.

As described previously, the FE models used damping factors obtained experimentally, which are presented in Table 4 to Table 9.

Table 4 Critical Damping Factors for S1P0.

Frequency [Hz]	Critical Damping Factor
699.64	0.00798
1343.91	0.01638
2264.00	0.03083

Table 5 Critical Damping Factors for S1P1.

Frequency [Hz]	Critical Damping Factor
704.42	0.00703
1338.62	0.01390
2025.52	0.01396

Table 6 Critical Damping Factors for S1P2.

Frequency [Hz]	Critical Damping Factor
705.94	0.00760
1348.84	0.01306
2046.24	0.01185

Table 7 Critical Damping Factors for S2P0.

Frequency [Hz]	Critical Damping Factor
683.02	0.00730
1317.94	0.01292
1995.14	0.02161

Table 8 Critical Damping Factors for S2P1.

Frequency [Hz]	Critical Damping Factor
689.59	0.00759
1309.59	0.01547
1986.76	0.02366

Table 9 Critical Damping Factors for S2P2.

Frequency [Hz]	Critical Damping Factor
691.34	0.00799
1325.12	0.01502
1997.59	0.01484

The vibration modes for the undamaged specimen and their respective non-damped natural frequencies are shown in Figure 6 and Table 10.

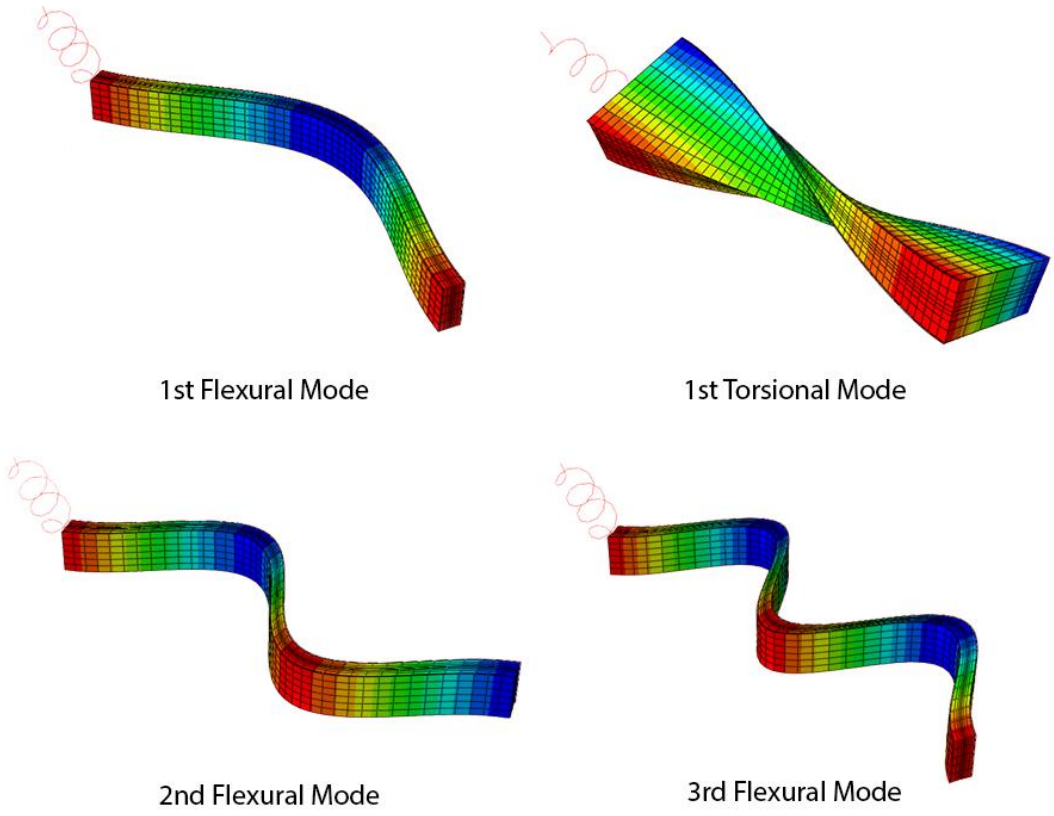

Figure 6: Non-rigid modal shapes for the undamaged sandwich structure.

Table 10 Modal Analysis– Numerical non-damped natural frequencies for specimen S1P0.

Mode	Frequency [Hz]
1st Flexural	780.96
1st Torsional	932.15
2nd Flexural	1402.30
3rd Flexural	2042.00

Based on the natural frequencies, as well as on the mode shapes and the obtained values for damping factors, the frequency range of interest was set for three first flexural modes ([50, 2300] Hz)). In fact, due to the used experimental set-up, it was not possible to obtain the damping factors for the torsional modes.

5.1 Case Study 1: Influence of the PZT Sensor

To verify the influence of the PZT sensor in the dynamic behavior of the sandwich structure, the FRF of the permanent accelerometer (Accelerometer 3) was compared to all specimens without damage. In other words, the FRFs came from specimens S1P0, S1P1 and S1P2. The results are shown in Figure 7 and Figure 8.

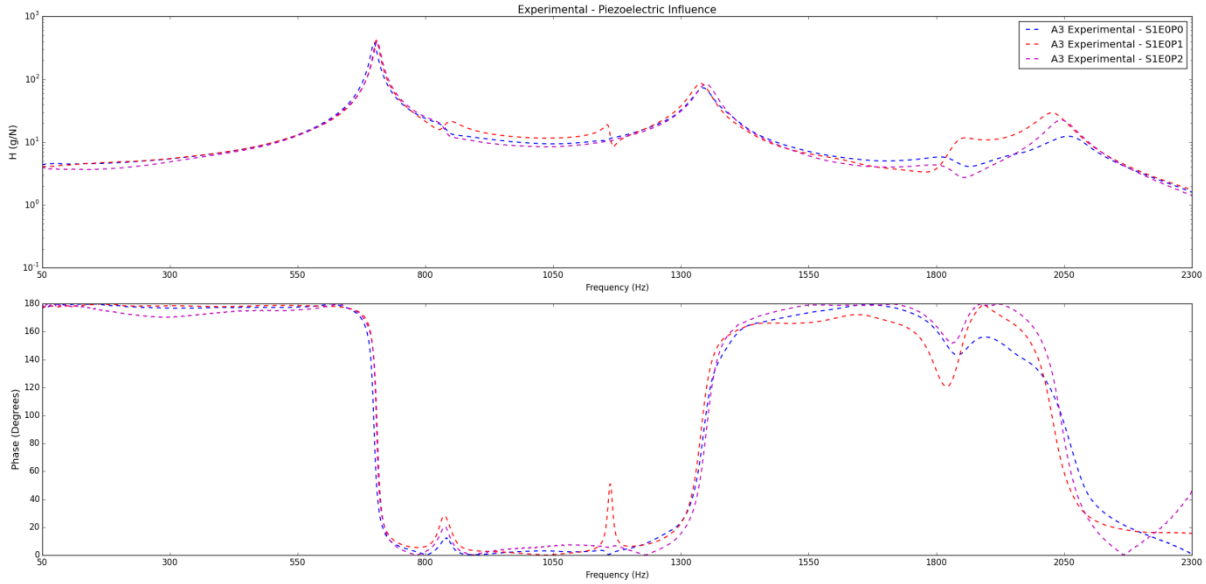

Figure 7: Experimental results: Influence of the PZT sensor in the dynamic response – A3.

By one hand, the influence of the MFC on the dynamic behavior of the sandwich structure is minimal as shown by the experimental results. By the other hand, the computational analysis showed a much greater influence of the MFC sensors.

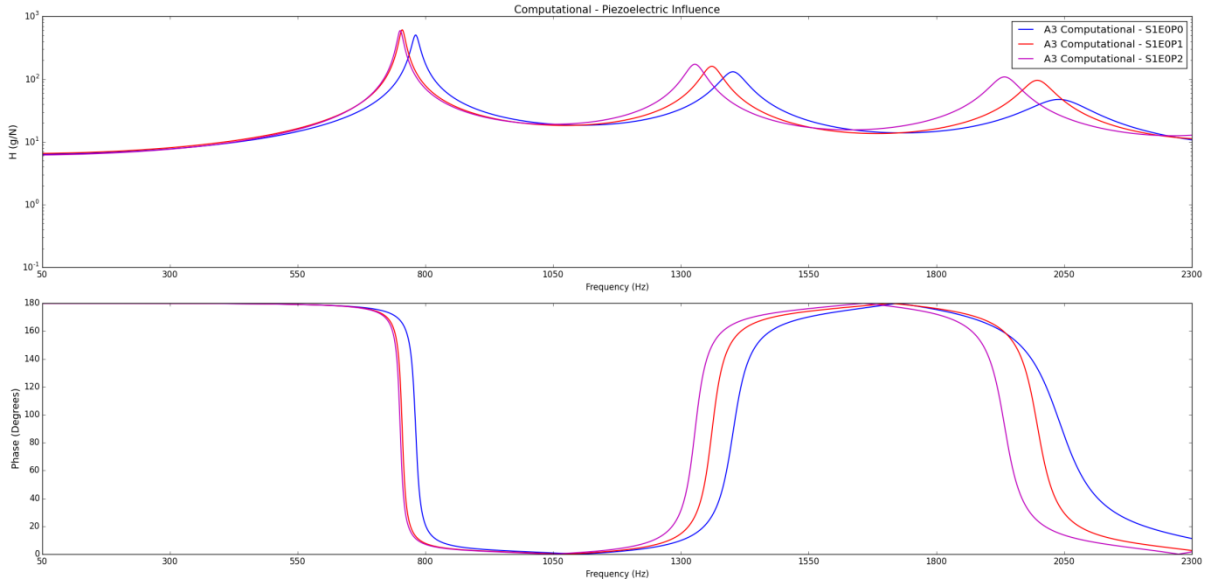

Figure 8: Computational results: Influence of the PZT sensor in the dynamic response – A3.

Comparing the experimental and computational curves of S1P0 in Figure 9, it becomes evident that the computational model displays higher stiffness values than the experimental specimens. One possible explanation is a discrepancy between the mechanical properties of the skins obtained from the literature and the real properties for the specimens used. By comparing the curves for specimen S1P2, it can be noticed that the computational analysis is also predicting higher influence of the MFC sensor than the influence obtained experimentally as shown by Figure 10.

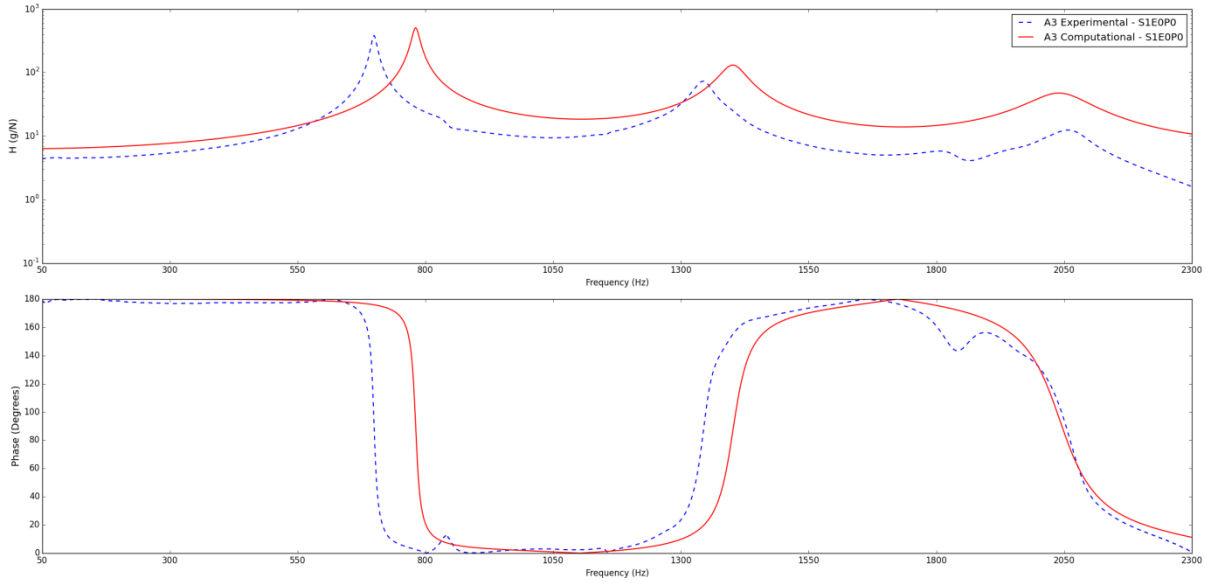

Figure 9: Computational *vs.* Experimental results for S1P0.

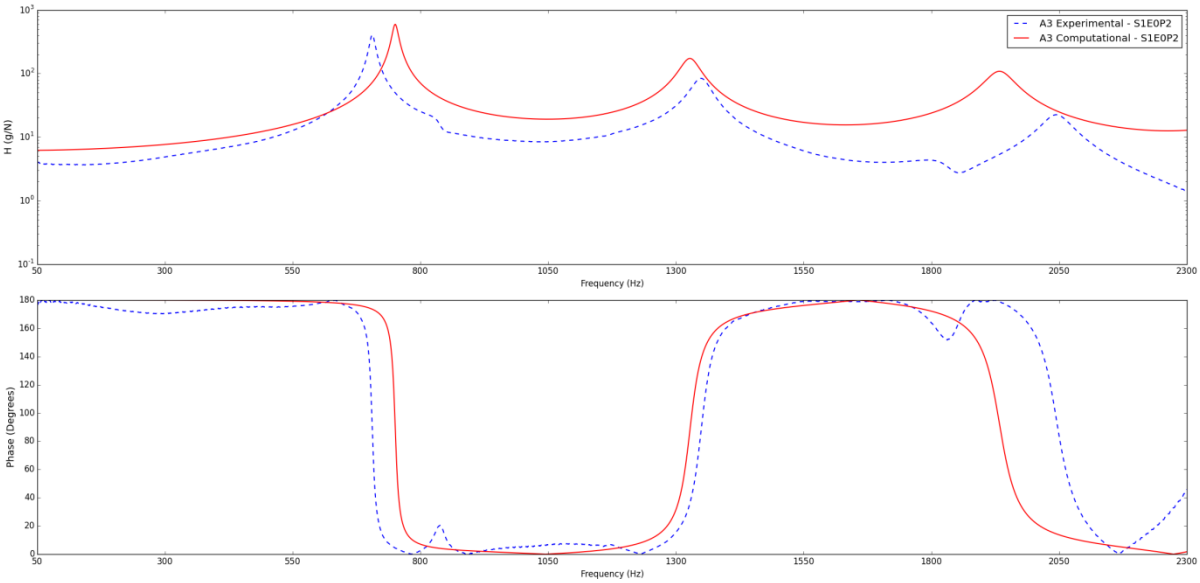

Figure 10: Computational *vs.* Experimental results for S1P2.

5.2 Case Study 2: Influence of the Damage

The influence of the debonding damage was studied by comparing the FRFs of the accelerometers for the specimens without MFC sensor. The reason for this investigation consists on isolating the influence of damage. Figure 11 shows the difference in FRF found experimentally.

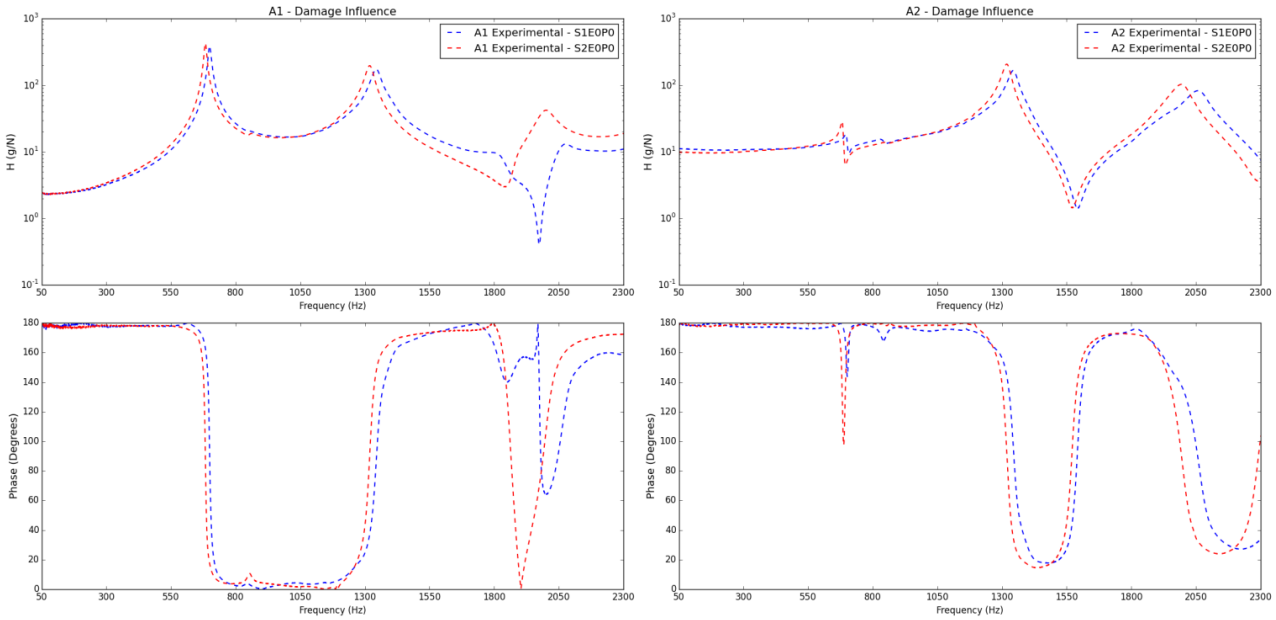

Figure 11: Experimental results: Influence of debonding damage - A1 and A2.

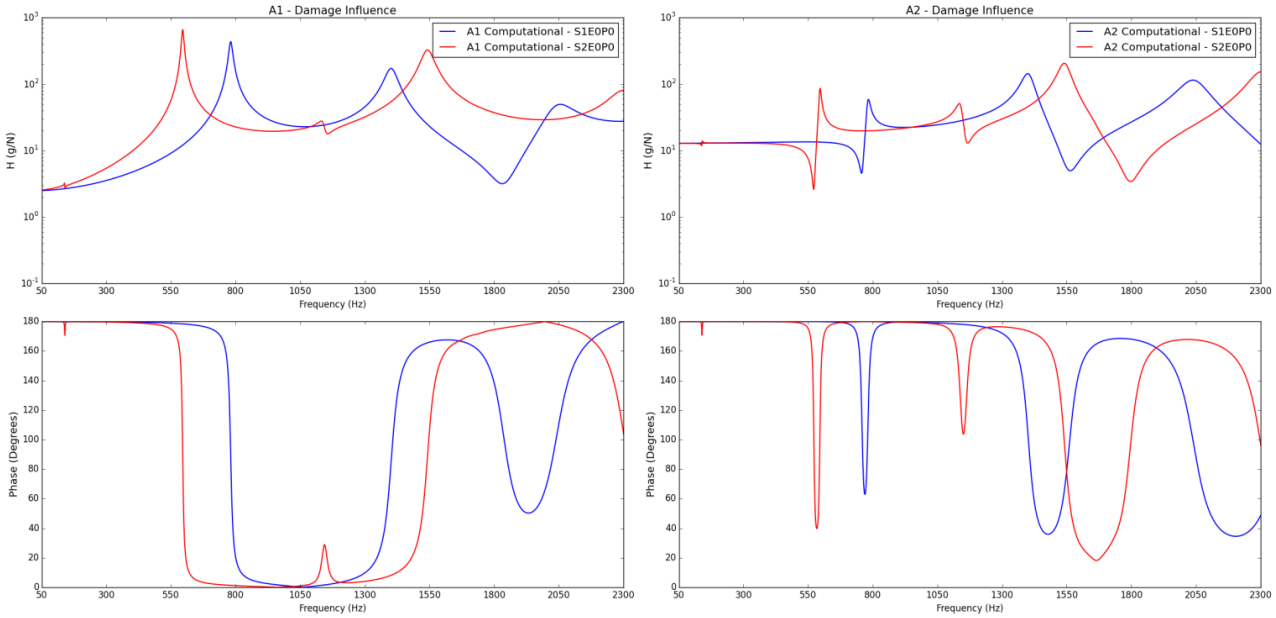

Figure 12: Computational results: Influence of debonding damage - A1 and A2.

Observing the responses for accelerometer 1 and 2, the influence of damage in the FE model, as seen in Figure 12, is much more relevant compared to experimental results. One possible reason for this effect is the absence of contact model in the modal computational analysis (steady state dynamic analysis), but this effect exists in the real debonded area. Thus, in the experiments, that same region might have resistance to movements due to the contact between the debonded surfaces. In addition, Figure 13 and Figure 14 show the experimental and computational results for accelerometer 3, and it is confirmed the same behavior.

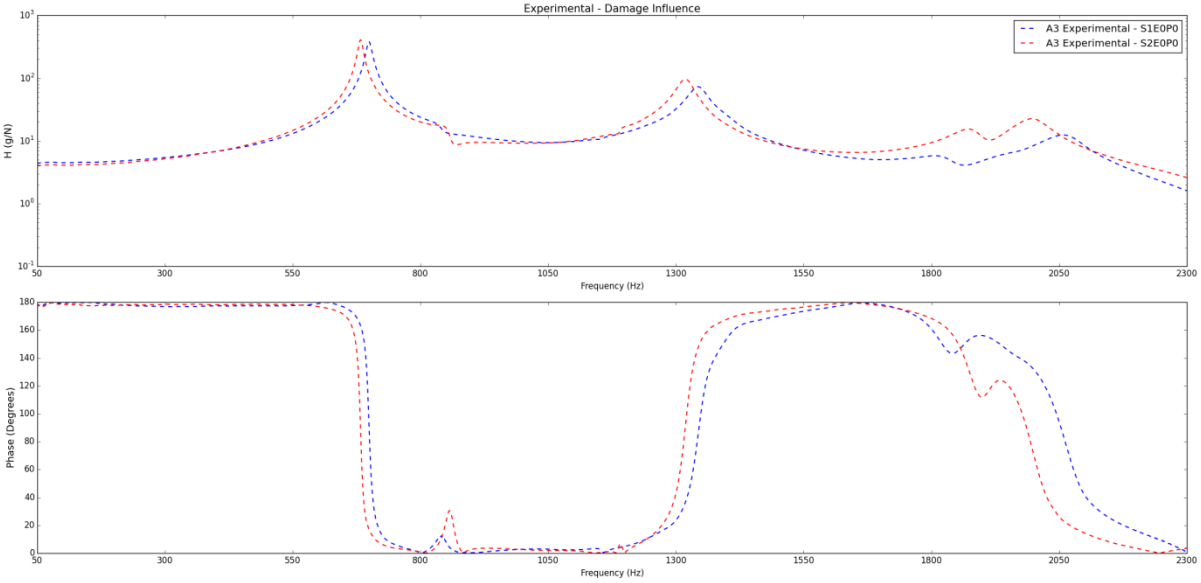

Figure 13: Experimental results: Influence of debonding damage - A3.

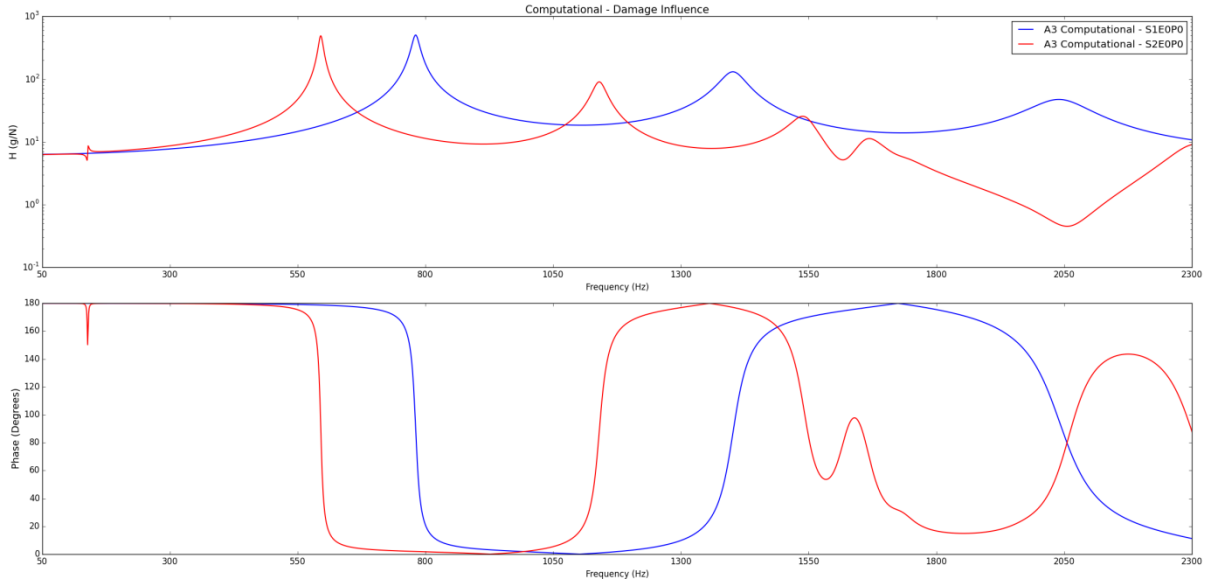

Figure 14: Computational results: Influence of debonding damage - A3.

5.3 Case Study 3: Damage Identification

The damage identification is performed by two different MFC sensors. The purpose of this case study consists on using the FRFs in order to observe the shift caused by the presence of damage, followed by damage metrics calculation.

The Frequency Response Functions used for these analyses are shown in Figure 15 and Figure 16.

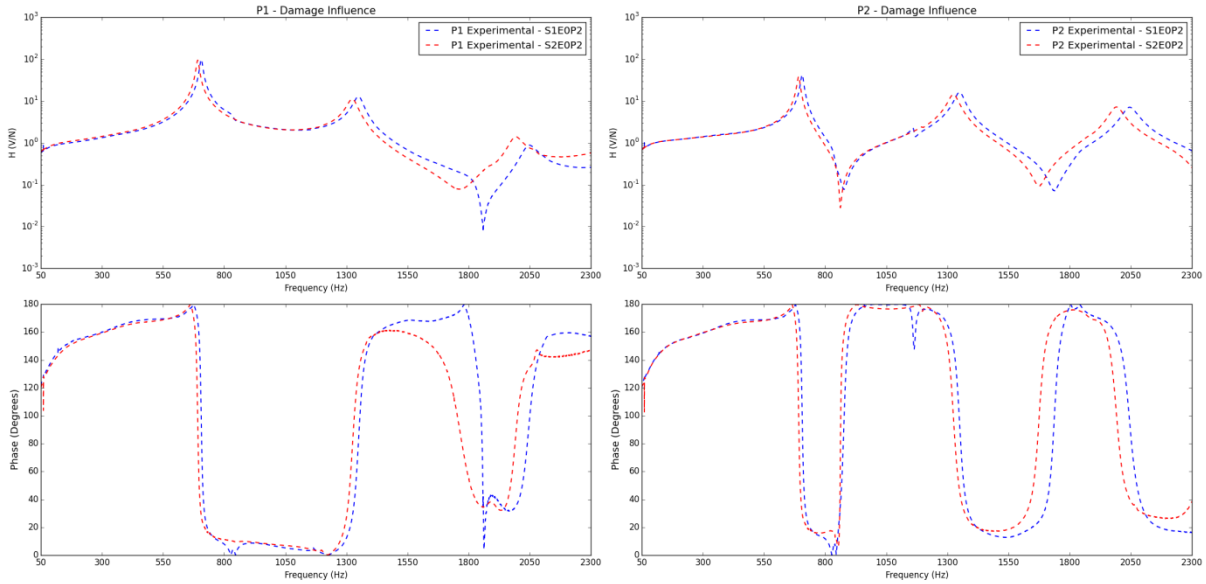

Figure 15: Experimental results: Influence of the damage - P1 and P2.

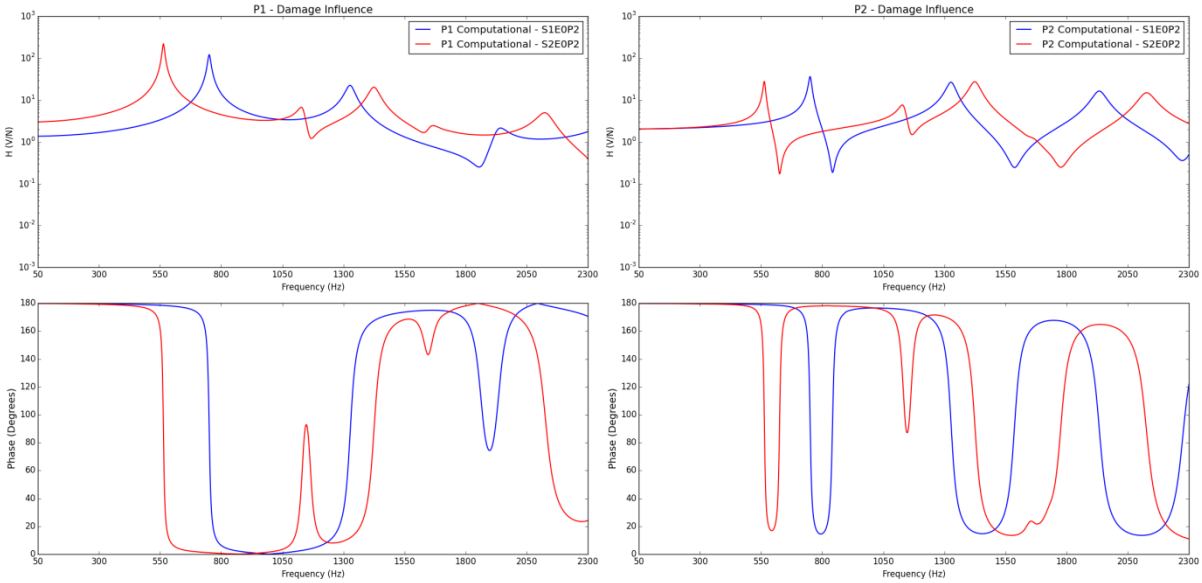

Figure 16: Computational results: Influence of the damage - P1 and P2.

As observed previously, the computational analysis did not properly represent the damage in the structure due to the absence of contact model for simulating the debonded region. Thus, the damage effect in the dynamic signature of the computational specimens is much greater than the experimental ones.

Figure 17 shows that for intact specimens (S1), the experimental and numerical dynamic signatures are slightly similar, where the highest differences are more evident for higher frequencies. However, as shown by Figure 18, the experimental and numerical responses of the damaged specimens are not close even for lower frequencies. This could be explained based on different aspects, such as the material properties of skins obtained from literature used in the FE model and the absence of contact model to simulate the debonded region. Besides, there is a high difference for the perfect adhesion between skins and core simulated by the FE model and the glued real region, which may have imperfect adhesion due to manufacturing issues.

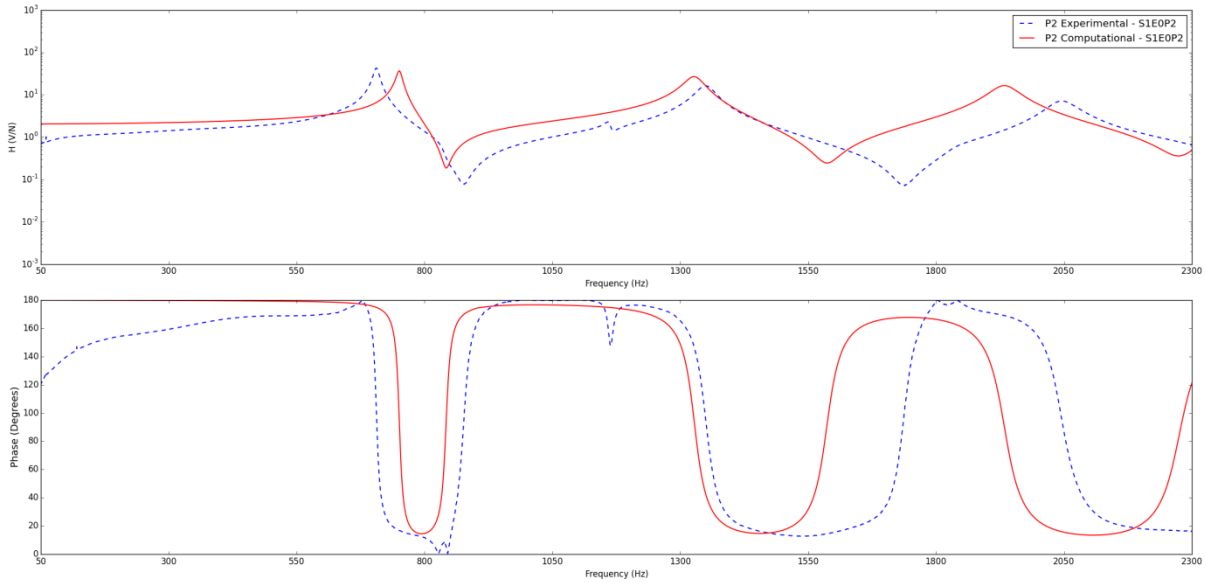

Figure 17: Computational *vs.* Experimental results for S1P2.

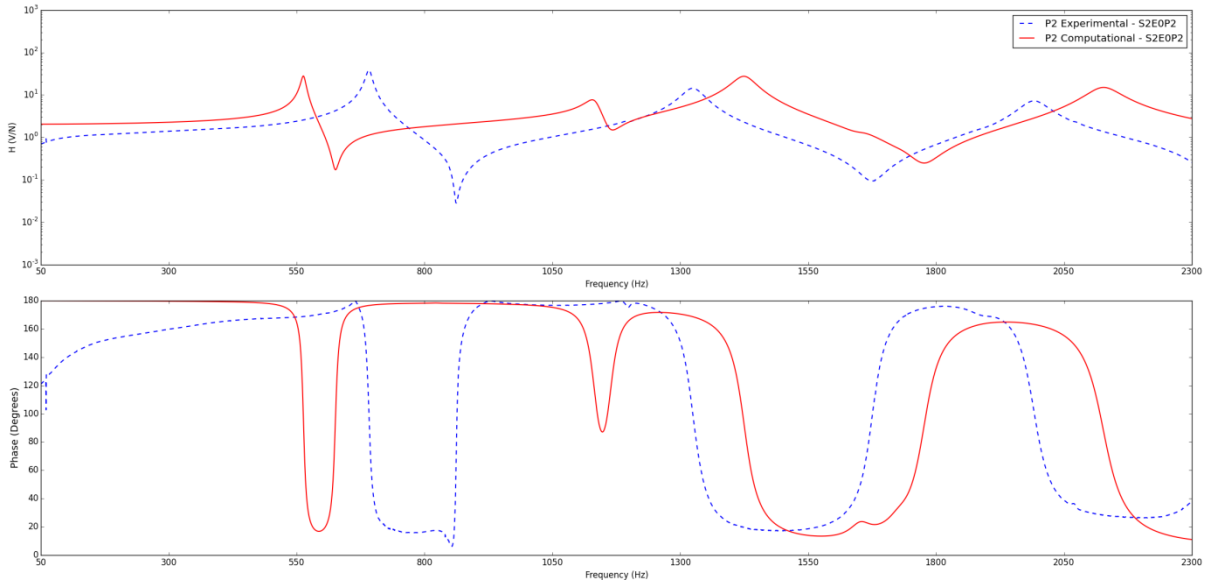

Figure 18: Computational *vs.* Experimental results for S2P2.

By applying the metrics of damage previously explained, it is possible to calculate the damage factors for the sandwich structures. The values are presented in Table 11 and Table 12. Considering Figure 1, H_{12} means input at position 1 and output at position 2, H_{13} means input at position 1 and output at position 3 and H_{15} means input at position 1 and output at position 5.

Table 11 Mickens' Damage Factors for the sandwich structures.

	No MFCs		**1 MFC**		**2 MFCs**	
Computational Model	**DF (Amplitude)**	**DF (Phase)**	**DF (Amplitude)**	**DF (Phase)**	**DF (Amplitude)**	**DF (Phase)**
H_{12}	2.41	1.75	1.99	0.73	0.86	8.30
H_{13}	1.66	0.59	0.87	9.24	2.01	1.58
H_{15}	0.88	12.72	2.2	11.71	1.78	1.35
Experiments						
H_{12}	1.41	0.76	0.20	0.11	0.44	0.79
H_{13}	0.25	0.14	0.26	0.65	0.66	0.65
H_{15}	0.35	0.46	0.47	0.52	0.39	0.36

Table 12 Damage Factors by using proposed procedure for the sandwich structures.

	No MFCs		**1 MFC**		**2 MFCs**	
Computational Model	**DF (Amplitude)**	**DF (Phase)**	**DF (Amplitude)**	**DF (Phase)**	**DF (Amplitude)**	**DF (Phase)**
H_{12}	0.27	0.25	0.31	0.24	0.30	0.41
H_{13}	0.34	0.25	0.31	0.46	0.26	0.27
H_{15}	0.30	0.47	0.25	0.32	0.32	0.34
Experiments						
H_{12}	0.12	0.10	0.09	0.08	0.08	0.10
H_{13}	0.10	0.11	0.08	0.10	0.06	0.11
H_{15}	0.09	0.09	0.07	0.12	0.10	0.11

Comparing Mickens' damage factors, it is possible to verify that the worst discrepancy in the values happened at H_{12} – Amplitude (Table 11), where the accelerometer indicates 1.41, and the MFC sensors indicated 0.20 and 0.44 for one and two sensors, respectively.

For the damage metrics obtained by using the proposed procedure, the damage factor obtained experimentally by the MFC 1 and MFC 2 were respectively 0.09 and 0.08 for H_{12} – Amplitude (Table 12). The damage factor obtained by A3 for a specimen without MFC sensor was of 0.12. The worst discrepancy of the modified damage factor calculation happens in the computational analysis for H_{13} – Phase with the MFC 1, which provides a damage factor of 0.46. And the accelerometer 3 shows a damage factor of 0.25.

Overall, the values were satisfactory, but the damage factors of the computational model became much greater than the experimental ones due to the effect of the debonding damage in the FRFs of the computational analyses caused by the absence of the contact model, as well as the influence of the material properties of the skins used in the FE model.

6 CONCLUSION

The damage metrics showed to be effective for damage identification in free-free sandwich structures. However, the metrics proposed by Mickens showed some discrepancies between values, and the proposed procedure in the present work was able to reduce the dispersion between the results. In addition, the use of MFC sensor response still represented a similar damage factor to

those of the reference accelerometers. Therefore, for SHM system is a good strategy to use the proposed procedure with MFC sensors.

For the computational models of the sandwich structures, debonding damage had stronger effect on the dynamic response compared to the experimental analyses. The discrepancy between the computational and the experimental results can be from problem during the manufacturing process to produce the damage (debonding area), so that there is an overestimation of the severity of damage in the finite element model compared to the real debonding extension in the structure. It is also difficult to control the process of gluing the skin to the core of the sandwich structure, while the computational model assumes a perfect link between them. Another source of discrepancy can be due to differences in material properties of the skins used in the computational model and the real ones. In addition, the absence of contact model in the modal computational analysis (steady state dynamic analysis) promotes a more flexible structure than the real one, when there is a debonded region. Therefore, the computational models should be certainly improved for future studies, considering not only material properties from characterization tests for all elements (skins, MFC sensor and core, including viscoelastic properties), but also the application of other finite element formulations.

7 ACKNOWLEDGEMENTS

The authors are thankful for the support of the National Council of Scientific and Technological Development (CNPq process number: 139806/2013-0 and 152445/2016-1), for funding this research. Volnei Tita would like to thank the financial support of the Air Force Office of Scientific Research – AFOSR (Grant FA9550-16-1-0222) and Sao Paulo Research Foundation (FAPESP).

REFERENCES

[1] NGUYEN, M. Q.; JACOMBS, S. S.; THOMSON, R. S.; HACHENBERG, D.; SCOTT, M. L.; (2005), “Simulation of impact on sandwich structures”, Composite Structures, v. 67, p. 217-227.

[2] LEIJTEN, J.; BERSEE, H. E. N.; BERGSMA, O. K.; BEUKERS, A.; (2009), “Experimental study of the low-velocity impact behaviour of primary sandwich structures in aircraft”, Composites: Part A, v.40, p. 164-175.

[3] DOEBLING, S.W.; FARRAR, C.R.; PRIME, M.B.; SHEVITZ, D.W., (1996), Damage identification and health monitoring of structural and mechanical systems from changes in their vibration characteristics: A literature review, page 2, Technical report, Los Alamos National Laboratory Report LA-13070-MS, Los Alamos, New Mexico.

[4] ORUGANTI, K., M. MEHDIZADEH, S. JOHN, AND I. HERSZBERG., (2009), “Vibration-based Analysis of Damage in Composites”. In The 2nd Asia-Pacific Workshop on Structural health Monitoring (2APWSHM), edited by S. Galea, W. Chiu, and A. Mita. Institute of Materials Engineering.

[5] YAM, L. H.; YAN, Y. J.; JIANG, J. S.; (2003), "Vibration-based damage detection for composite structures using wavelet transform and neural network identification", Composite Structures, v. 60, p. 403-412.

[6] LUCHINSKY, D. G.; Hafiychuk, V.; Smelyanskiy, V.; Tyson, R. W.; Walker, J. L.; Miller, J. L.; (2011), "High-fidelity modeling for health monitoring in honeycomb sandwich structures", In: Aerospace Conference, IEEE. p. 1-7.

[7] LESTARI, W., QIAO, P., (2005), "Damage detection of fiber-reinforced polymer honeycomb sandwich beams", Composite Structures, v. 67, n. 3, p. 365-373.

[8] AMIR, S., MORLIER, J., GOURINAT, Y, (2010), "Damage monitoring in sandwich beams by modal parameter shifts: A comparative study of burst random and sine dwell vibration testing", Journal of Sound and Vibration, v. 329, no. 5, p. 566-584.

[9] DHAMANDE, L. S., BHASKAR, R. V., (2014), "Damage Detection in Aluminium Honeycomb Structure using Vibration Analysis", International Journal of Current Engineering and Technology, v.5 n.5.

[10] SINGH, C.V. AND TALREJA, R., (2010), "Evolution of ply cracks in multidirectional composite laminates", International Journal of solids and structures, v. 47. pp. 1338-1349.

[11] TITA, V., CALIRI JUNIOR, M. F., (2012), "Numerical Simulation of Anisotropic Polymeric Foams", Latin American Journal of Solids and Structures, pp 1 -21.

[12] CALIRI JUNIOR, M. F., SOARES, G. P., ANGELICO, R. A., CANTO, R. B., TITA, V., (2012), "Study of an Anisotropic Polymeric Cellular Material Under Compression Loading", Materials Research, 15(3), pp 359 – 364.

[13] TITA, V., CALIRI JUNIOR, M. F., ANGELICO, R. A., CANTO, R. B., (2012), "Experimental Analyses of the Poly(vinyl chloride) Foams' Mechanical Anisotropic Behavior", Polymer Engineering and Science, v. 52, pp. 2654-2663

[14] SARTORATO, M., MEDEIROS, R., TITA, V., (2015), "A finite element formulation for smart piezoelectric composite shells: Mathematical formulation, computational analysis and experimental evaluation", Composite Structures, v. 127, p. 185-198.

[15] MEDEIROS, R. "Development of a criterion for predicting residual strength of composite structures damaged by impact loading. Tese de Doutorado - Escola de Engenharia de São Carlos, Universidade de São Paulo, São Carlos, 2015.

[16] FLOR, F. R. Monitoramento do dano em estruturas de material compósito através de métodos baseados em vibrações: juntas coladas metal-compósito e estruturas sanduíche. Dissertação de Mestrado - Escola de Engenharia de São Carlos, Universidade de São Paulo, São Carlos, 2015.

[17] MICKENS, T., SCHULZ, M., SUNDARESAN, M., GHOSHAL, A., NASER, A. AND REICHMEIDER, R., (2003), "Structural health monitoring of an aircraft joint", Mechanical Systems and Signal Processing, v. 17, No. 2, pp. 285 – 303.

RESPONSIBILITY NOTICE

The authors are the only responsible for the printed material included in this paper.

MecSol 2017 – 6th International Symposium on Solid Mechanics
Joinville, SC - Brazil, April 26-28, 2016

STRUCTURAL HEALTH MONITORING FOR SANDWICH STRUCTURES

Denys E. T. Marques[1], Felipe R. Flor[1], Ricardo de Medeiros[2], Carlos C. Pagani Junior[1], Volnei Tita[1]*

[1] Aeronautical Engineering Department, São Carlos School of Engineering, University of Sao Paulo, Sao Carlos, Sao Paulo, Brazil

[2] Mechanical Engineering Department, College of Technological Sciences, Santa Catarina State University, Joinville, Brazil

*Corresponding author: voltita@sc.usp.br

Abstract: This work aims to contribute for the development of SHM systems based on vibration methods to be applied on sandwich structures. The main objective is focused on the damage identification. Specimens of a sandwich structure made of skins in epoxy resin reinforced by glass fiber and a core of PVC foam are manufactured. First, finite element models are developed in order to analyze the dynamic characteristics of undamaged and damaged structures with presence or not of two piezoelectric sensors. Then, vibration experimental analyses are performed on undamaged specimens of sandwich structures. The mode shapes and natural frequencies are compared to the computational results. Second, vibration experimental analyses are carried out on undamaged and damaged specimens of sandwich structures with piezoelectric sensors or not. Finally, a traditional damage metric is calculated based on Frequency Response Functions obtained from computational and experimental analyses. However, this work brings a new procedure in order to improve the quality of results provided by this damage metric. By one hand, the damage metric values showed that the new procedure is effective to identify the damage using both amplitude and phase experimental data. By the other hand, for computational analysis, the damage metric values are not effective, because the finite element models were not able to simulate the dynamic behavior of the sandwich structures.

Keywords: Structural Health Monitoring, Sandwich Structures, Vibration Methods, Finite Element Analysis, Experimental Analysis.